
ACCURACY OF THE PLANAR COMPLIANT MECHANISMS

MUSTAFA HASAN, LJUBOMIR LILOV

In the recent years a class of devices called compliant mechanisms is in the focus of many investigations. Their use in the design of modern devices, especially in micro-electro-mechanical systems (MEMS), is inevitable because of the difficulty in fabricating rigid-body joints and assembling parts. Compliant mechanisms rely upon elastic deformation to perform their function of transmitting and/or transforming motion and force. Flexural pivot-based designs use narrow sections connecting relatively rigid segments. Thus, compliance is lumped to a few portions of the mechanism. The introduction of the elastic pivots instead of the rigid-body joints leads to certain deviations in the performance of the compliant mechanisms compared with the analogous rigid-body linkages. These deviations are the object of study in the paper. Based on the graph theory, a method for effective estimation of the accuracy of compliant mechanisms with flexural pivots is elaborated and practical examples are considered.

Keywords: Accuracy, Compliant Mechanisms, Flexure Hinges.

2000 MSC: 70B15

1. INTRODUCTION

The definition of *compliant mechanisms* can be found in the literature, based either on the output motion, or on their design. Compliant mechanisms derive a part or whole of the relative motion between its members from intentional elastic deformation of the members rather than from conventional rigid body kinematic pairs alone [1]. A compliant mechanism can be also defined, as a single-piece flexible structure that delivers the desired motion by undergoing elastic deformation as opposed to the rigid body motions in a conventional mechanism [2].

Such mechanisms may be considered for use in a particular application for a variety of reasons. The advantages of compliant mechanisms are considered in two categories: cost reduction (part-count reduction, reduced assembly time, and simplified manufacturing processes) and increased performance (increased precision, increased reliability, reduced wear, reduced weight, and reduced maintenance).

Generally, the categories of compliant mechanisms can be divided into three kinds:

- Fully compliant mechanisms.
- Compliant mechanisms in which only the joints are compliant.
- Compliant mechanisms in which only the links are compliant.

Our interest is in the second one, in which the flexure hinges (flexure pivots) act as of joints. A flexure hinge is a thin member that provides the relative rotation between two adjacent rigid members through flexing (bending) where a conventional rotational joint is compared to a flexure hinge [3]. Flexure hinge is a typical simple and ingenious mechanical structure. Being made up of a monolithic material, it possesses many outstanding properties which ordinary hinge does not have, and can satisfies the demands for high accuracy and stability measurement and movement [4].

The flexure hinges are incorporated in a large number of applications, both civil and military, including translation micro-positioning stages, piezoelectric actuators and motors, high-accuracy alignment devices for optical fibers, missile-control devices, displacement amplifiers, robotic micro-displacement mechanisms and so on. Recently, increasing applications of monolithic flexure hinge mechanism have been made to guide motions with precision. Micro-motion stages utilizing the flexure hinge mechanism can have many advantages: negligible backlash and stick-slip friction, smooth and continuous displacement, adequate for magnifying the output displacement of actuation, and inherently infinite resolution [5].

One kind of the flexure hinges is called super elastic hinges. These hinges are made of a super elastic material such as shape memory alloy (SMA) having an effect of super elasticity, so that they have the capacity to perform large bending displacements [6].

Generally, the accuracy of a mechanical system is the quality of the system characterizing closeness of the results of the execution of certain operations by the mechanical system to the result of the execution of the same operations by the ideal mechanical system. In this paper the performance of mechanism with super elastic hinges is compared with the performance of mechanism with normal joints, considered as an ideal system. A mathematical model and compact analytical expressions allowing the exact estimation of the deflections in link positions of the mechanism with super elastic hinges are presented. Widely used mechanisms are considered as examples for application of the theory presented.

2. MATRIX DESCRIPTION OF THE INTERCONNECTION STRUCTURE

Let us consider a planar mechanism consisting of $n + 1$ links interconnected by m rotational hinges. We replace each rotational hinge by a super elastic plate and in this way we arrive to a mechanism with compliance for which the interconnection structure of the links is the same but the hinges are not more rotational pairs. The deviation in the position of an arbitrary link of the new (compliant) mechanism in the absolute plane with respect to the position of the same link of the primary (rigid) mechanism is the object of study in the paper.

There are always two basic links in each real mechanism: the stationary base (fixed link or frame) and another link, which plays a special role in the mechanism and performs a preliminary given motion. This is the motion for which the mechanism is actually designed. This link is called characteristic link. In the formalism developed further each link can be considered as a characteristic one if its motion is of special interest. The fixed link will be considered as a link number 0 and the characteristic link gets number i^* . The fixed link together with the characteristic link determine the basic open chain (possibly not the only one) in the mechanism. This basic chain is unambiguously determined for some mechanisms like industrial robots and manipulators but for others the basic chain may be chosen under some possibilities. The links belonging to the basic chain get numbers $1, 2, \dots, i^*$ starting from the link next to the fixed link.

We represent the mechanism structure by a graph, whose vertices s_i ($i = 0, 1, \dots, n$) and edges u_a ($a = 1, \dots, m$) symbolize respectively the links and the hinges of the system. The labeling of the links and vertices, as well as the hinges and edges is identical and it will be clear from the context when there is a question of link or vertex, respectively of hinge or edge. We are talking about rotational pair and more generally about hinge when two links are interacting directly, i.e. each rotational pair (hinge) connects exactly two links. The three links given in Fig. 1 sharing one rotational axis define in this way two rotational pairs.

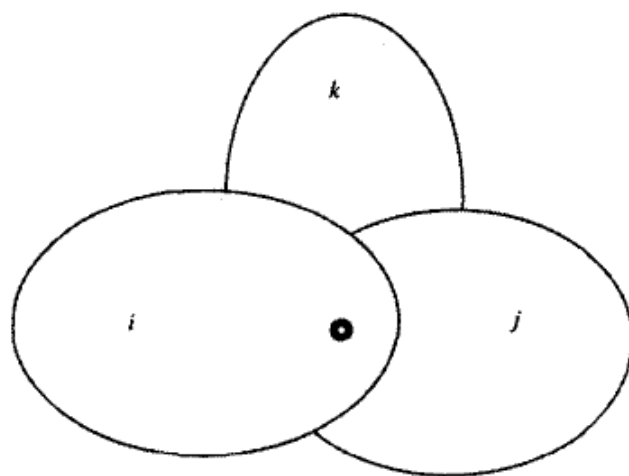


Fig. 1

The edge of the basic chain, which is incident with the vertex number i ($i = 1, \dots, i^*$) gets the same number. The system graph is generally an arbitrary graph and its transformation into a graph with a tree-like structure (so called *skeleton tree*) can be reduced to the removing of $\hat{n} = m - n$ appropriately selected edges from the graph. We assume that the removed edges do not belong to the basic chain. In the tree obtained each pair of vertices is connected with one and only one simple chain in which every vertex appears only one time. We label the vertices in such a way, that the numbers of the vertices belonging to each simple chain beginning from the vertex s_0 form a monotonously increasing sequence. Such labeling is called *regular*. In this labeling the numbers from 1 to n are assigned to the edges of the skeleton tree in such a way that one of the two vertices connected by the edge number a has the same number $i = a$ and besides, this edge belongs to the simple chain connecting s_0 with s_i . The nonskeleton edges get numbers from $(n + 1)$ to m . The simple chains which connect the vertices of the skeleton tree s_i with the vertex s_0 will be called *direct paths* and denoted by the symbol $[s_0, s_i]$ [7].

When describing the relative motion in the hinge number a it must be specified unambiguously which motion relative to which link is meant. As a basic link when describing the relative motion in hinge number a we choose the link with the smaller number. After the choice is completed we can define two functions $i^+(a)$ and $i^-(a)$ ($a = 1, \dots, m$) where $i^+(a)$ means the number of the reference link and $i^-(a)$ is the number of the contiguous link. From the chosen rule of links labeling it follows obviously that $i^-(a) = a$ for $a = 1, 2, \dots, n$. By introducing the functions $i^+(a)$ and $i^-(a)$ we obtain the possibility to give a sense of direction to every edge and in this way to transform it to arc assuming that $i^+(a)$ is the number of the vertex from which the arc u_a is pointing away, and $i^-(a)$ is the number of the vertex toward which the arc u_a is pointing. The graph obtained is called *oriented graph*.

One of the basic matrices describing the structure of the introduced graphs is the *incidence matrix* of the oriented graph $\underline{I} = (S_{ia})$ ($i = 0, 1, \dots, n, a = 1, \dots, m$), where

$$S_{ia} = \begin{cases} 1 & \text{if } i = i^+(a), \\ -1 & \text{if } i = i^-(a), \\ 0 & \text{otherwise,} \end{cases} \quad (2.1)$$

i.e. $S_{ia} = 1$, if the arc u_a starts at a vertex s_i , $S_{ia} = -1$, if the arc u_a ends at the vertex s_i and $S_{ia} = 0$ otherwise [8]. Obviously each column of the incidence matrix contains exactly one element $+1$ and one element -1 because exactly two vertices define each arc. The incidence matrix allows reconstructing entirely the system graph and describes in this way unambiguously the system structure.

We introduce also the matrix $\underline{I}^+ = (S_{ia}^+)$ ($i = 0, 1, \dots, n; a = 1, \dots, m$) according to the rule

$$S_{ia}^+ = \begin{cases} 1 & \text{if } i = i^+(a), \\ 0 & \text{otherwise.} \end{cases} \quad (2.2)$$

This matrix is gained, obviously, from the matrix \underline{I} replacing in it all -1 through zero.

Let us represent now the incidence matrix in the form

$$\underline{I} = \begin{bmatrix} \underline{\check{S}}_0 & \underline{\hat{S}}_0 \\ \underline{\check{S}} & \underline{\hat{S}} \end{bmatrix} = \begin{bmatrix} \underline{S}_0 \\ \underline{S} \end{bmatrix},$$

where:

$$\begin{aligned} \underline{\check{S}}_0 &= (S_{0a}) \quad (a = 1, \dots, n); & \underline{\hat{S}}_0 &= (S_{0a}) \quad (a = n + 1, \dots, m); \\ \underline{S}_0 &= (S_{0a}) \quad (a = 1, \dots, m); & \underline{\check{S}} &= (S_{ia}) \quad (i, a = 1, \dots, n); \\ \underline{\hat{S}} &= (S_{ia}) \quad (i = 1, \dots, n; a = n + 1, \dots, m); \\ \underline{S} &= (S_{ia}) \quad (i = 1, \dots, n; a = 1, \dots, m). \end{aligned}$$

Another important matrix is the *fundamental loops matrix (cyclomatic matrix)* $\underline{\Phi}$ [8]. Let $\Phi_{n+1}, \Phi_{n+2}, \dots, \Phi_m$ be the fundamental loops determined by the nonskeleton arcs $u_{n+1}, u_{n+2}, \dots, u_m$. We choose the direction of the arc u_{n+i} as a positive direction in the loop Φ_{n+i} . The cyclomatic matrix is determined then as a $\hat{n} \times m$ -matrix $\underline{\Phi} = (\varphi_{n+i,b})$ ($i = 1, \dots, \hat{n}, b = 1, \dots, m$) in the following way:

$$\varphi_{n+i,b} = \begin{cases} 1, & \text{if } u_b \in \Phi_{n+i} \text{ and has the direction of } u_{n+i}, \\ -1, & \text{if } u_b \in \Phi_{n+i} \text{ and has the opposite direction of } u_{n+i}, \\ 0, & \text{otherwise.} \end{cases} \quad (2.3)$$

The last structure matrix we introduce is the *matrix of direct paths* $\underline{\Psi} = (\psi_{ai})$ ($a = 1, \dots, m; i = 1, \dots, n$) [7], where

$$\psi_{ai} = \begin{cases} 1 & \text{if } u_a \in [s_0, s_i] \text{ and is directed towards } s_0, \\ -1 & \text{if } u_a \in [s_0, s_i] \text{ and is directed from } s_0, \\ 0 & \text{otherwise.} \end{cases}$$

This matrix has the form

$$\underline{\Psi} = \begin{bmatrix} \underline{T} \\ \underline{0}_{\hat{n} \times n} \end{bmatrix}; \quad \hat{n} = m - n, \quad \underline{T} = \underline{\check{S}}^{-1}, \quad \underline{T} = (\tau_{ai}) \quad (a, i = 1, \dots, n)$$

because of the introduced regular labeling. Here and further $\underline{0}_{k \times s}$ denotes matrix with all elements equal to zero.

Let us consider as a first example the four-bar mechanism with coupler point presented in Fig. 2. The four-bar linkage is the simplest possible closed-loop mechanism, and has numerous uses in industry and for simple devices found in automobiles, toys, etc. The device gets its name from its four distinct links (or

bars). Link 0 is the ground link (the frame or fixed link), and is assumed to be motionless. Links 1 and 3 each rotate relative to the ground link about fixed pivots (A_0 and B_0). Link 2 is called coupler link, and is the only link a point C of which can trace paths of different shape (because the link is not rotating about a fixed pivot). Usually one of the “grounded links” (link 1 or 3) serves as the input link, which is the link which may either be turned by hand, or perhaps driven by an electric motor or a hydraulic or pneumatic cylinder.

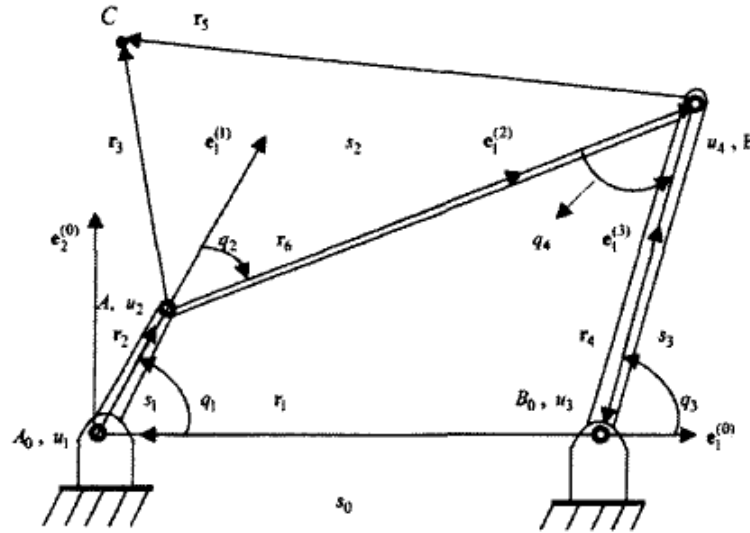


Fig. 2. Four-bar mechanism with coupler point C

For the given mechanism one possible choice of the functions $i^+(a)$ and $i^-(a)$ is represented in the following table

a	1	2	3	4
$i^+(a)$	0	1	0	2
$i^-(a)$	1	2	3	3

The corresponding oriented graph is given in Fig. 3.

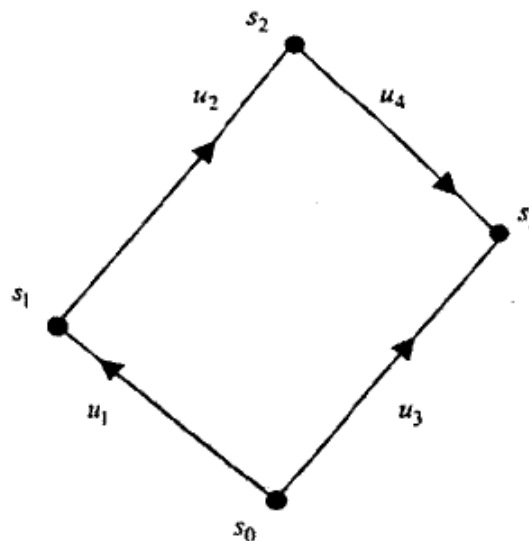


Fig. 3. Graph of the four-bar mechanism

The structure matrices \underline{I} , $\underline{\Phi}$ and $\underline{\Psi}$ have the form, respectively:

$$\underline{I} = \begin{bmatrix} 1 & 0 & 1 & 0 \\ -1 & 1 & 0 & 0 \\ 0 & -1 & 0 & 1 \\ 0 & 0 & -1 & -1 \end{bmatrix}, \quad \underline{\Phi} = [1 \quad 1 \quad -1 \quad 1], \quad \underline{\Psi} = \begin{bmatrix} -1 & -1 & 0 \\ 0 & -1 & 0 \\ 0 & 0 & -1 \\ 0 & 0 & 0 \end{bmatrix}.$$

As a second example we consider the six-bar Stephenson-I mechanism (Fig. 4).

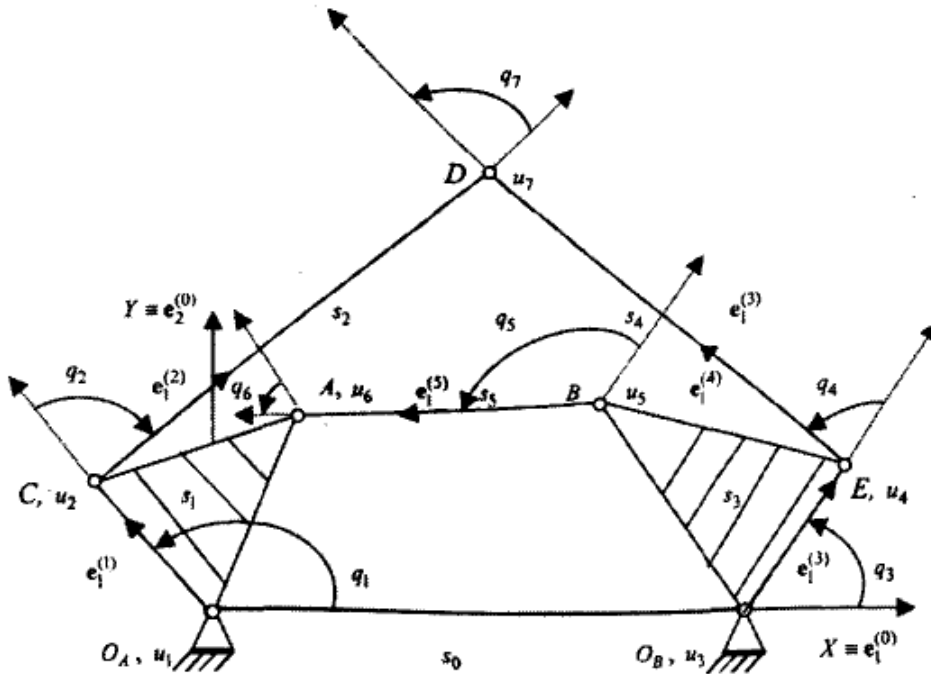


Fig. 4. Six-bar Stephenson-I mechanism with coordinate systems

The six-bar mechanism is considered as a multibody system consisting of six bodies (including the frame) interconnected with seven revolute joints as shown in Fig. 4. The moving links are numbered from 1 to 5 while the frame gets the number 0. The joints are numbered from 1 to 7. One possible choice of the functions $i^+(a)$ and $i^-(a)$ is given through the following table

a	1	2	3	4	5	6	7
$i^+(a)$	0	1	0	3	3	1	2
$i^-(a)$	1	2	3	4	5	5	4

The graph of the six-bar mechanism is a cyclic graph (Fig. 5). It can be reduced to a graph with a tree-like structure by cutting exactly two appropriately chosen arcs, for instance u_6 and u_7 .

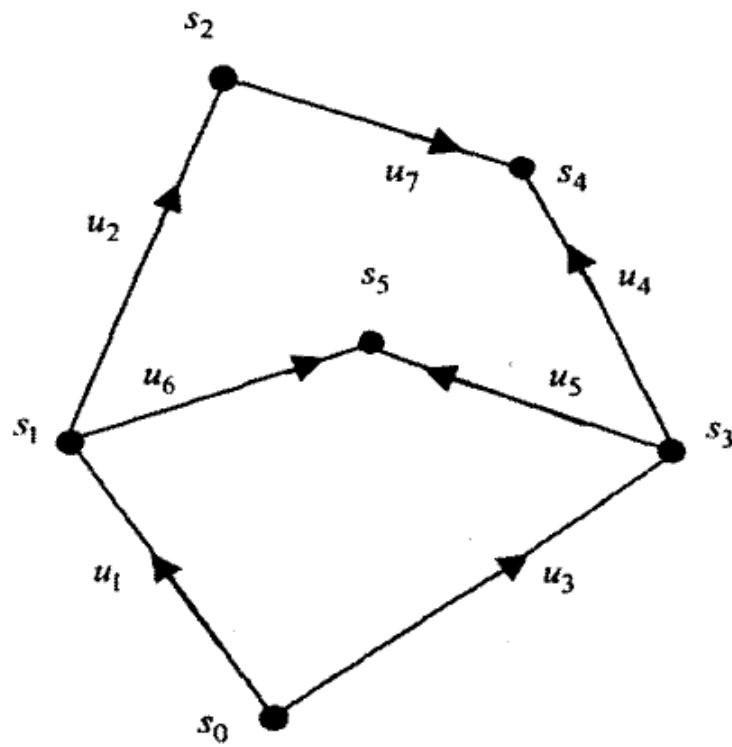


Fig. 5. Graph of the six-bar mechanism

The structure matrices have the form:

$$\underline{I} = \begin{bmatrix} 1 & 0 & 1 & 0 & 0 & 0 & 0 \\ -1 & 1 & 0 & 0 & 0 & 1 & 0 \\ 0 & -1 & 0 & 0 & 0 & 0 & 1 \\ 0 & 0 & -1 & 1 & 1 & 0 & 0 \\ 0 & 0 & 0 & -1 & 0 & 0 & -1 \\ 0 & 0 & 0 & 0 & -1 & -1 & 0 \end{bmatrix}, \quad \underline{\Phi} = \begin{bmatrix} 1 & 0 & -1 & 0 & -1 & 1 & 0 \\ 1 & 1 & -1 & -1 & 0 & 0 & 1 \end{bmatrix},$$

$$\underline{\Psi} = \begin{bmatrix} -1 & -1 & 0 & 0 & 0 \\ 0 & -1 & 0 & 0 & 0 \\ 0 & 0 & -1 & -1 & -1 \\ 0 & 0 & 0 & -1 & 0 \\ 0 & 0 & 0 & 0 & -1 \\ 0 & 0 & 0 & 0 & 0 \\ 0 & 0 & 0 & 0 & 0 \end{bmatrix}.$$

The last example is the mechanism shown in Fig. 6 with nine links and ten revolute joints (planar platform).

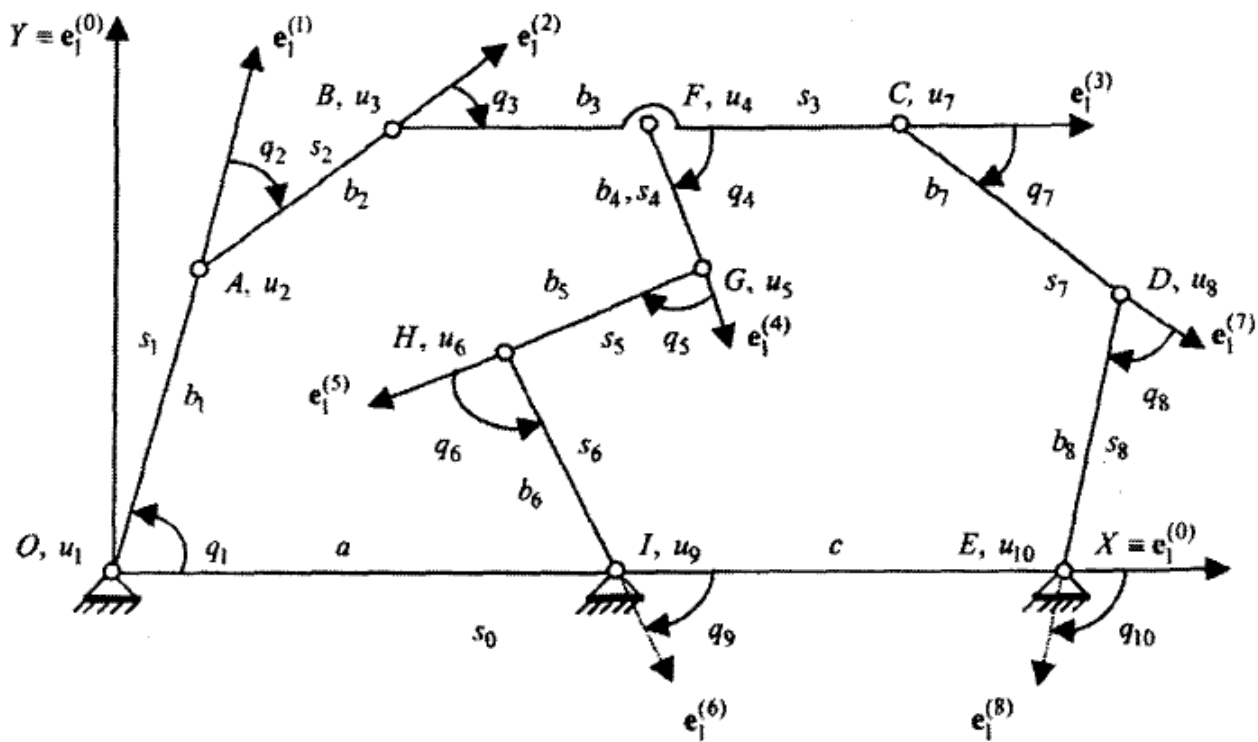


Fig. 6. Nine-bar mechanism with the coordinate systems

One possible choice of the functions $i^+(a)$ and $i^-(a)$ is given in the following table:

a	$i^+(a)$	$i^-(a)$
1	0	1
2	1	2
3	2	3
4	3	4
5	4	5
6	5	6
7	3	7
8	7	8
9	0	6
10	0	8

The corresponding oriented graph is given in Fig. 7.

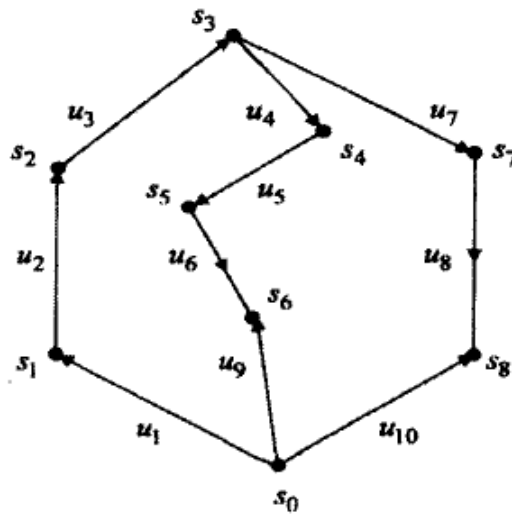


Fig. 7. Graph of the nine-bar mechanism

The graph of the mechanism is a cyclic graph and can be reduced to a graph with a tree-like structure by cutting exactly two appropriately chosen arcs, for instance u_9 and u_{10} . The corresponding structure matrices have the following form:

$$\underline{I} = \begin{bmatrix} 1 & 0 & 0 & 0 & 0 & 0 & 0 & 0 & 1 & 1 \\ -1 & 1 & 0 & 0 & 0 & 0 & 0 & 0 & 0 & 0 \\ 0 & -1 & 1 & 0 & 0 & 0 & 0 & 0 & 0 & 0 \\ 0 & 0 & -1 & 1 & 0 & 0 & 1 & 0 & 0 & 0 \\ 0 & 0 & 0 & -1 & 1 & 0 & 0 & 0 & 0 & 0 \\ 0 & 0 & 0 & 0 & -1 & 1 & 0 & 0 & 0 & 0 \\ 0 & 0 & 0 & 0 & 0 & -1 & 0 & 0 & -1 & 0 \\ 0 & 0 & 0 & 0 & 0 & 0 & -1 & 1 & 0 & 0 \\ 0 & 0 & 0 & 0 & 0 & 0 & 0 & -1 & 0 & -1 \end{bmatrix},$$

$$\underline{\Phi} = \begin{bmatrix} -1 & -1 & -1 & -1 & -1 & -1 & 0 & 0 & 1 & 0 \\ -1 & -1 & -1 & 0 & 0 & 0 & -1 & -1 & 0 & 1 \end{bmatrix}$$

$$\underline{\Psi} = \begin{bmatrix} -1 & -1 & -1 & -1 & -1 & -1 & -1 & -1 \\ 0 & -1 & -1 & -1 & -1 & -1 & -1 & -1 \\ 0 & 0 & -1 & -1 & -1 & -1 & -1 & -1 \\ 0 & 0 & 0 & -1 & -1 & -1 & 0 & 0 \\ 0 & 0 & 0 & 0 & -1 & -1 & 0 & 0 \\ 0 & 0 & 0 & 0 & 0 & -1 & 0 & 0 \\ 0 & 0 & 0 & 0 & 0 & 0 & -1 & -1 \\ 0 & 0 & 0 & 0 & 0 & 0 & 0 & -1 \\ 0 & 0 & 0 & 0 & 0 & 0 & 0 & 0 \\ 0 & 0 & 0 & 0 & 0 & 0 & 0 & 0 \end{bmatrix}$$

In link number i ($i = 0, 1, \dots, n$) we chose a coordinate system $O_i x_i y_i z_i$ in the following way. The axis z_i is the rotation axis of link i with respect to the previous

link in the direct path from s_0 to s_i . All axes z_i are parallel and orthogonal to the common motion plain of the links. If the link number i is an inner one for the skeleton tree and besides it is connected with one or more following links with numbers j, k, \dots, l ($j < k < \dots < l$), then the axis x_i is a common normal of z_i and z_j in the motion plain, directed towards z_j . The axis x_i intersects the axes z_i and z_j in points O_i and O_j , respectively. We chose the first point as an origin of the coordinate system $O_i x_i y_i z_i$ in which the axis y_i lays in the motion plane and complements the axes x_i and z_i to right-hand system. Analogously, on each of the axes belonging to the link i with numbers $j < k < \dots < l$ points O_j, O_k, \dots, O_l are defined (Fig. 8).

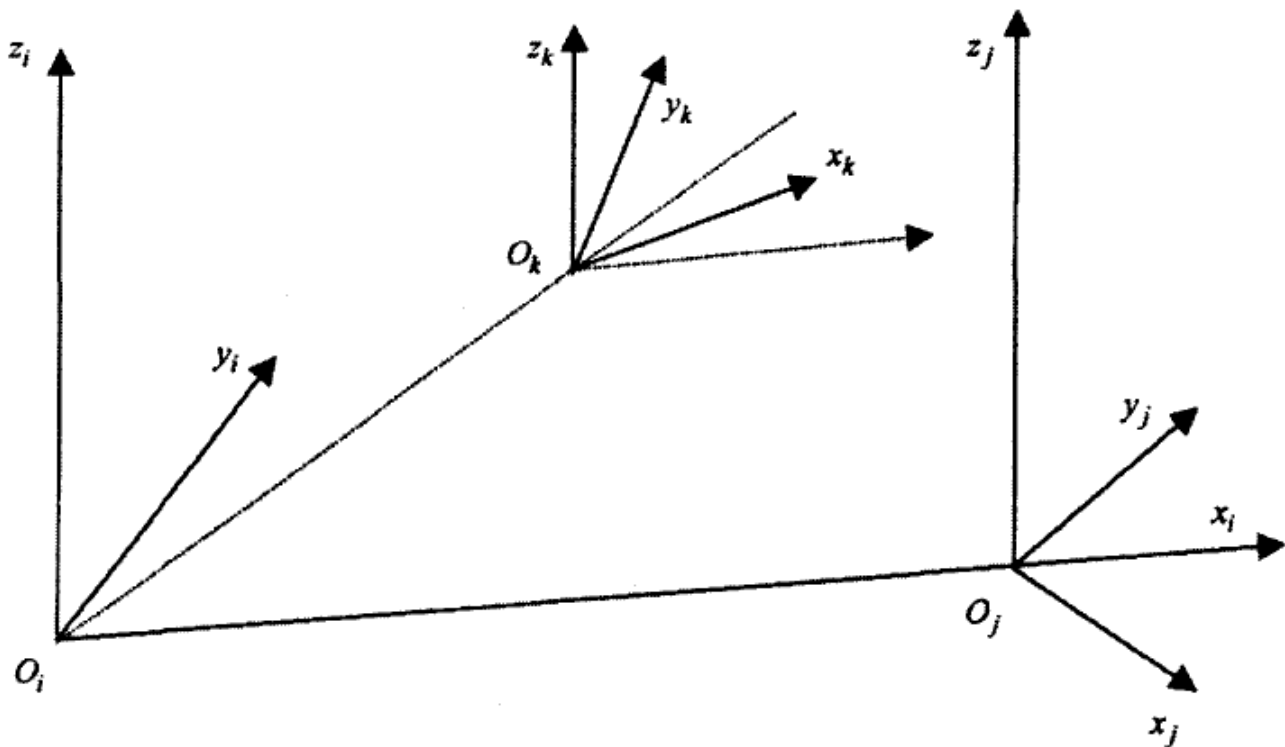


Fig. 8

In the peripheral links the axes x and y of the coordinate systems are chosen arbitrarily but so that they built right-hand systems with the rotation axis z of the peripheral link with respect to the previous one. In the fixed (zero) link the axis z_0 is chosen to coincide with the axis z_1 and the axes x_0 and y_0 are chosen arbitrarily. In addition to the coordinate system $O_i x_i y_i z_i$ in each of the links except the zero one we will use a coordinate system with an origin in an arbitrarily chosen point C_i of the link and parallel axes with unit vectors $\mathbf{e}_1^{(i)}, \mathbf{e}_2^{(i)}, \mathbf{e}_3^{(i)}$. The position of the link $i^-(a)$ with respect to the link $i^+(a)$ we determine with the angle q_a between the x -axes of the coordinate systems $C_i \mathbf{e}^{(i)}$ introduced, $q_a = \angle(\mathbf{e}_1^{i^+(a)}, \mathbf{e}_1^{i^-(a)})$.

Let us replace now the revolute hinges in the motion plane through thin plates with lengths l_a having super elasticity, while the system is in a certain position \underline{q}^* . We assume that the rotation centers R_a are located at the centers of the lengths

of the elastic hinges and that the lengths of the plates are small quantities $l_a \ll 1$ (Fig. 9).

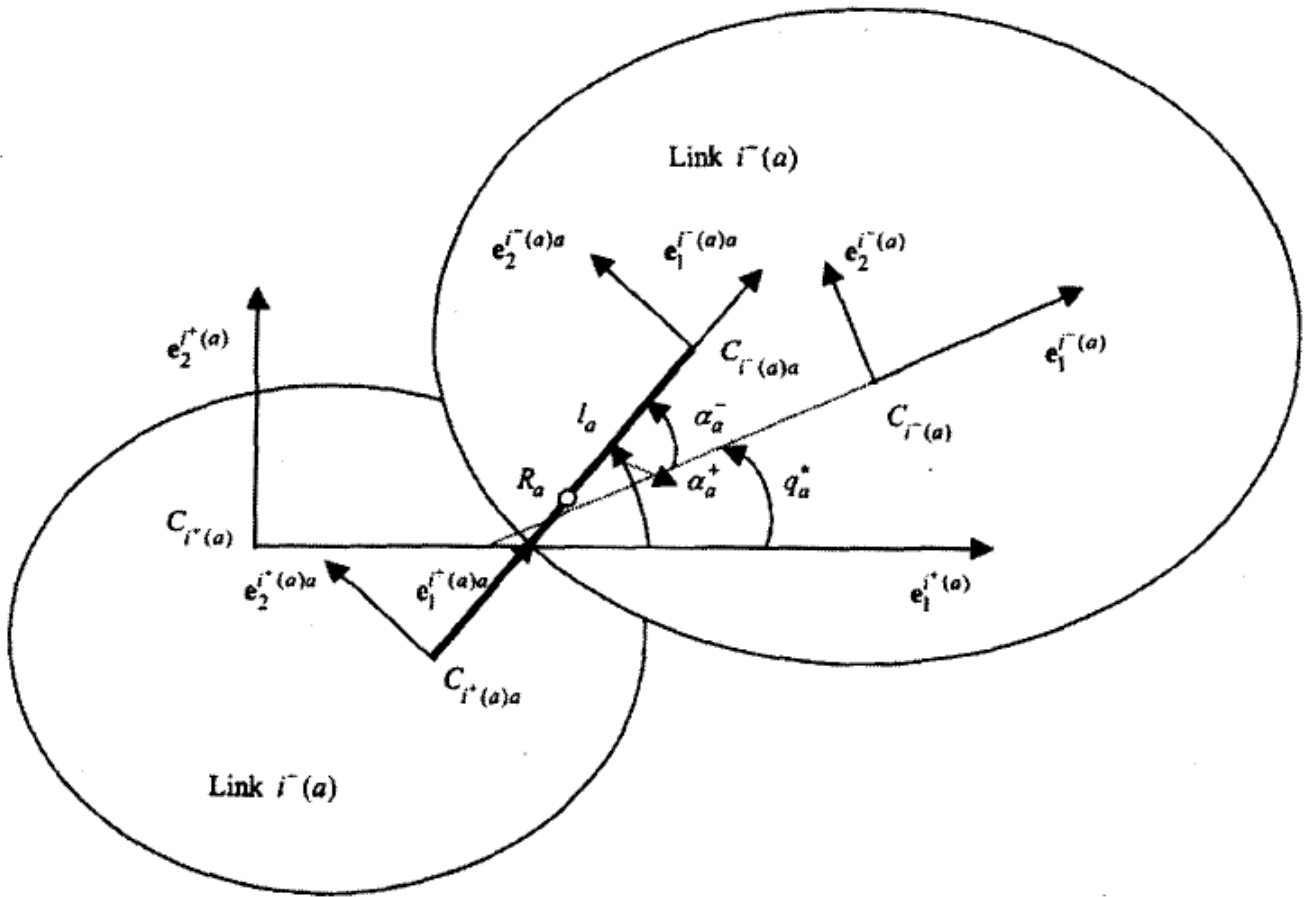


Fig. 9

3. RELATIVE DEVIATION

The basic considerations begin with the description of the relative motions in the hinges. The relative positions of the links will be determined by a method that is more complex than it is necessary when considering only a mechanism with rotational (rigid) hinges, but the method is equally applicable to the both mechanisms. This approach gives us the opportunity to realize the desired comparison. For this purpose for each hinge two *hinge points* $C_{i^\pm(a)a}$ in the corresponding contiguous links are specified and the *hinge vector* $\mathbf{z}_a = \overline{C_{i^+(a)a}C_{i^-(a)a}}$ is introduced. We denote the radius vectors of the hinge points $C_{i^\pm(a)a}$ in the corresponding bases by $\mathbf{c}_{ia} = \overline{C_i C_{ia}}$ ($i = i^\pm(a)$, $a = 1, \dots, m$) (Fig. 10). In order to describe the relative motion in hinge a we introduce in each of the contiguous links additional reference frames $C_{i^\pm(a)a}\mathbf{e}^{(i^\pm(a)a)}$ rigidly attached to the corresponding links $i^\pm(a)$. The position of the system $C_{i^\pm(a)a}\mathbf{e}^{(i^\pm(a)a)}$ with respect to $C_{i^\pm(a)}\mathbf{e}^{(i^\pm(a))}$ is determined by the position of its origin $C_{i^\pm(a)a}$ and the angle α_a^\pm , $\alpha_a^+ = \angle(\mathbf{e}_1^{i^+(a)}, \mathbf{e}_1^{i^+(a)a})$, $\alpha_a^- = \angle(\mathbf{e}_1^{i^-(a)}, \mathbf{e}_1^{i^-(a)a})$. We choose as hinge points the ends of the super elastic

plate. The axes $\mathbf{e}_1^{i^+(a)a}$ and $\mathbf{e}_1^{i^-(a)a}$ are directed along the plate when it is in undeformed state in position q^* and then they remain fixed in the corresponding links (Fig. 9, Fig. 10, Fig. 11, Fig. 12).

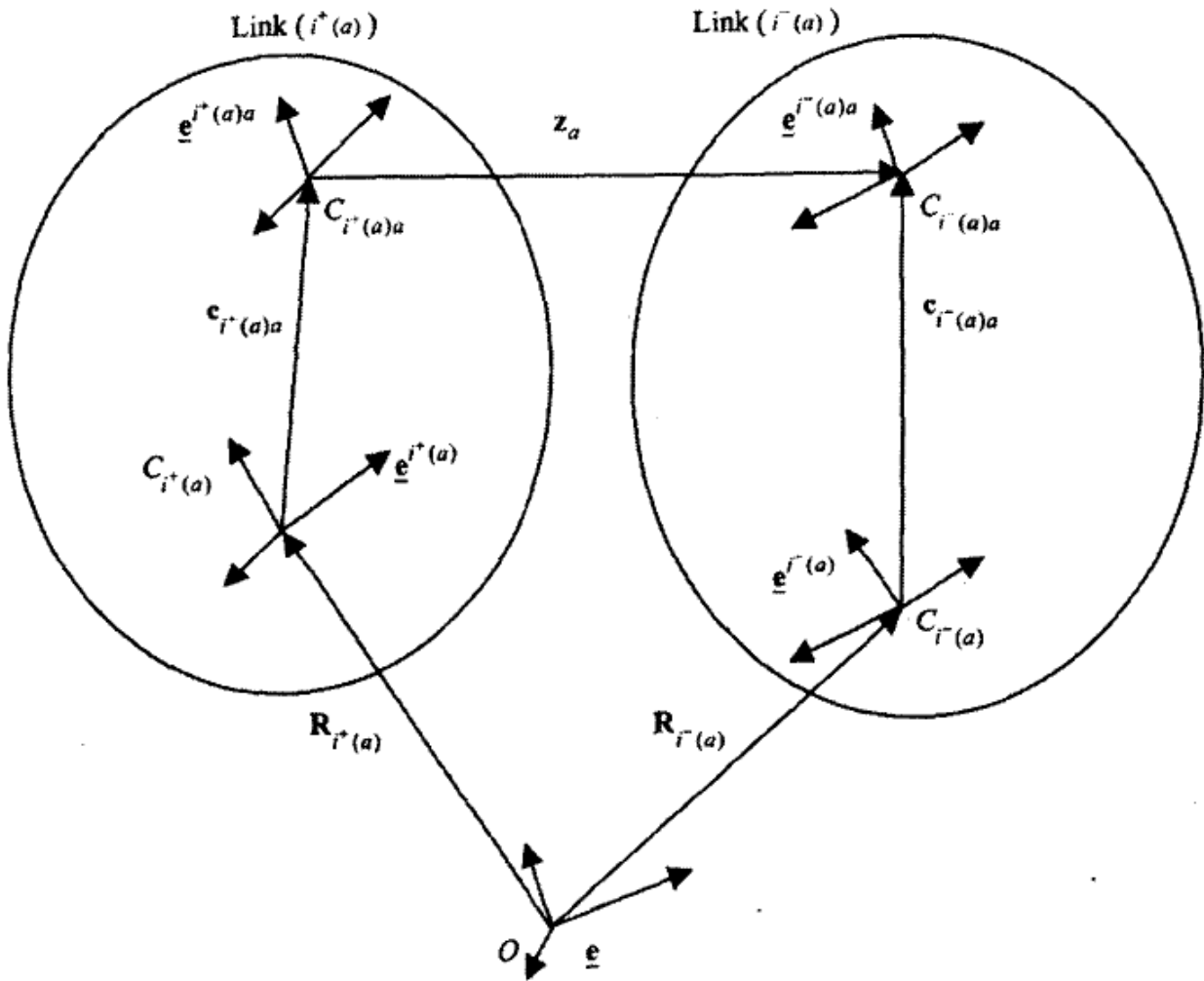


Fig. 10

The vector \mathbf{z}_a and the basis $\underline{\mathbf{e}}^{i^-(a)}$ are functions of the chosen parameter of the relative motion in hinge number a , i.e.

$$\mathbf{z}_a = \mathbf{z}_a(q_a), \quad \underline{\mathbf{e}}^{(i^-(a))} = \underline{\mathbf{e}}^{(i^-(a))}(q_a).$$

The position of the plate itself in undeformed state with respect to the coordinate systems in the contiguous bodies is determined by the angles $\alpha_a^+ \angle (\mathbf{e}_1^{i^+(a)}, \mathbf{e}_1^{i^+(a)a})$ and $\alpha_a^- \angle (\mathbf{e}_1^{i^-(a)}, \mathbf{e}_1^{i^-(a)a})$ (Fig. 9). For the initial (rigid) mechanism the relative motion in hinge a is a rotation around the center R_a which is the middle of the plate and the vector \mathbf{z}_a has the form (Fig. 12)

$$\begin{aligned} \mathbf{z}_a^r &= \overline{C_{i^+(a)a} C_{i^-(a)a}} = \overline{C_{i^+(a)a} R_a} + \overline{R_a C_{i^-(a)a}} \\ &= \left(\frac{l_a}{2} + \frac{l_a}{2} \cos q_a \right) \mathbf{e}_1^{i^+(a)a} + \left(\frac{l_a}{2} \sin q_a \right) \mathbf{e}_2^{i^+(a)a}. \end{aligned} \quad (3.1)$$

Here and further the index (*r*) (from rigid) is used for quantities connected with the initial (rigid) mechanism. For the corresponding quantities of the mechanism obtained after replacing the rotational hinges through super elastic plates we will use designations without index.

The relative motion in hinge number *a* is realized by virtue of the elastic deformation of the plate which replaces the rotation pair. The position of the system $C_{i^-(a)a} \mathbf{e}_1^{i^-(a)a}$ with respect to the system $C_{i^+(a)a} \mathbf{e}_1^{i^+(a)a}$ is determined through the angle $\theta_a = \angle (\mathbf{e}_1^{i^+(a)a}, \mathbf{e}_1^{i^-(a)a})$ (Fig. 11, Fig. 12).

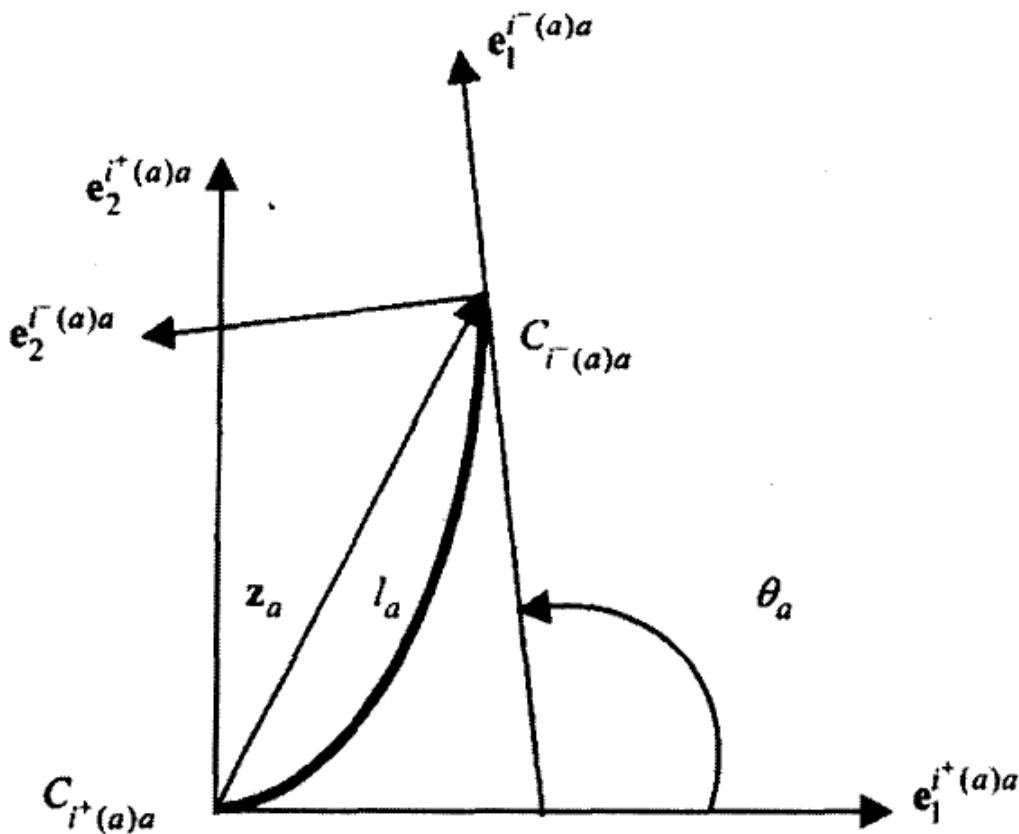


Fig. 11

Let q_a mean in the elastic mechanism again the angle $\angle (\mathbf{e}_1^{i^+(a)a}, \mathbf{e}_1^{i^-(a)a})$. The following relationship is evident (Fig. 11, Fig. 12, Fig. 13):

$$q_a = \alpha_a^+ + \theta_a - \alpha_a^- = \theta_a + q_a^*.$$

The links of the both mechanisms in an undeformed state when $\theta_a = 0$ take identical position q^* in the absolute frame.

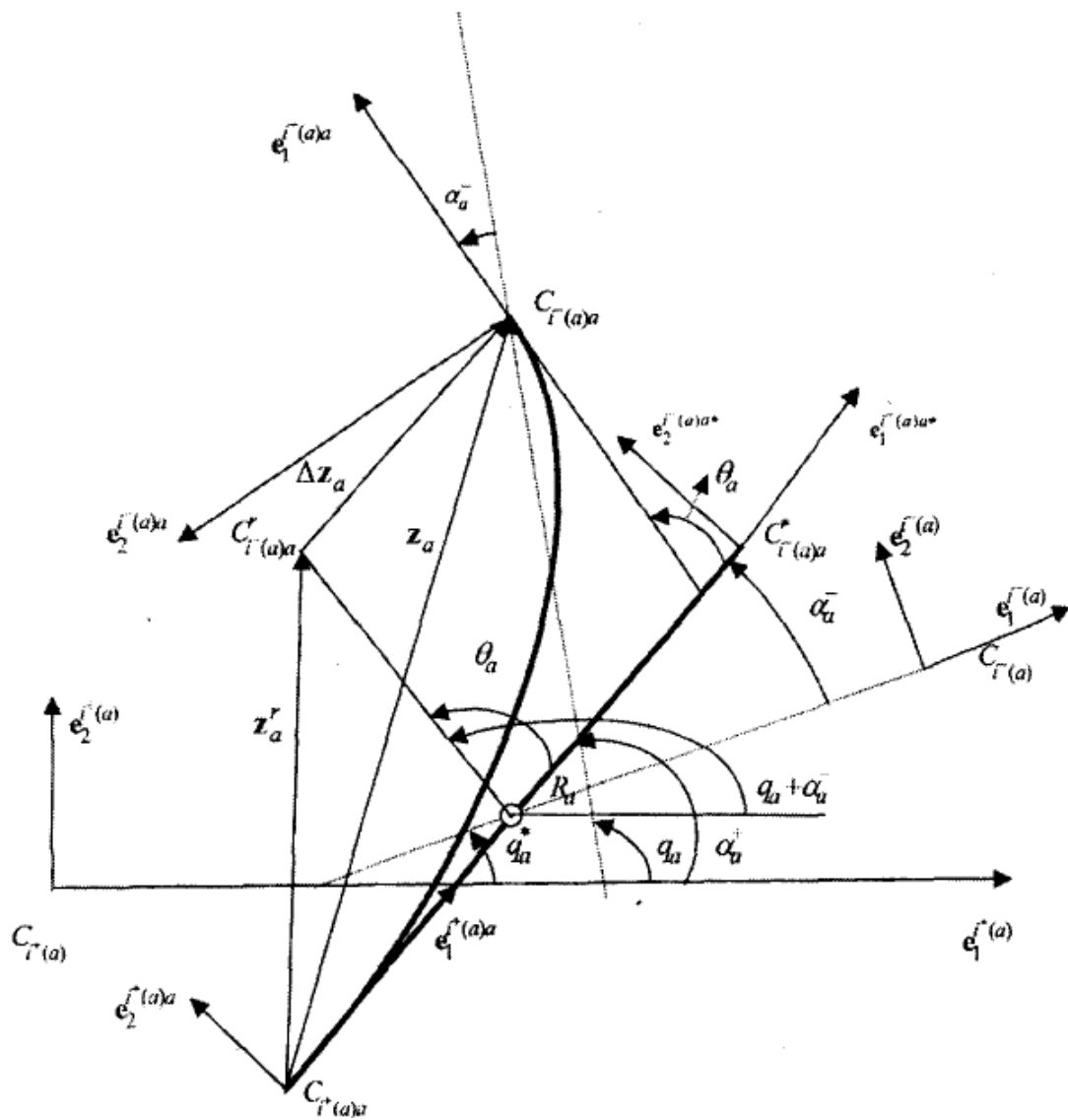


Fig. 12

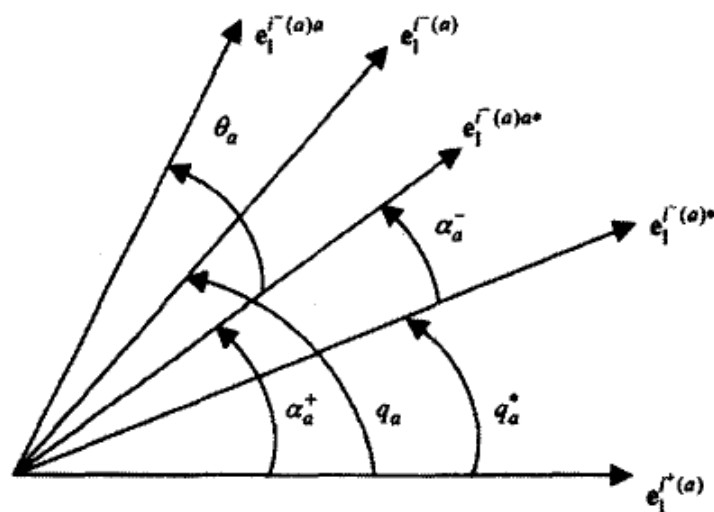


Fig. 13

We assume that the form of the deformed plate is determined through the angle θ_a . Then the translational displacement \mathbf{z}_a of the coordinate system $C_{i^-(a)a} \mathbf{e}^{i^-(a)a}$

with respect to the coordinate system $C_{i+(a)a}\mathbf{e}^{i+(a)a}$ can be written down in the form

$$\mathbf{z}_a = \overline{C_{i+(a)a}C_{i-(a)a}} = f_a(\theta_a)\mathbf{e}_1^{i+(a)a} + g_a(\theta_a)\mathbf{e}_2^{i+(a)a}, \quad (3.2)$$

where functions $f_a(\theta_a)$ and $g_a(\theta_a)$ are known through the equation of the neutral line of the deformed plate found theoretically or from the experiment. The deviation to be determined between the links of the elastic mechanism with respect to the links of the initial mechanism is the difference between (3.1) and (3.2) (Fig. 12):

$$\begin{aligned} \Delta\mathbf{z}_a &= \mathbf{z}_a - \mathbf{z}_a^r = \\ &= \left[f_a(\theta_a) - \left(\frac{l_a}{2} + \frac{l_a}{2} \cos q_a \right) \right] \mathbf{e}_1^{i+(a)a} + \left[g_a(\theta_a) - \frac{l_a}{2} \sin q_a \right] \mathbf{e}_2^{i+(a)a}. \end{aligned} \quad (3.3)$$

4. DEVIATION OF THE COMPLIANT MECHANISM

We choose as an absolute coordinate system $O\mathbf{e}$ (reference frame) the coordinate system in the fixed (zero) link $O_0\mathbf{e}^0$. The position of each link of the mechanism in this system is determined with the help of the radius-vector \mathbf{R}_i of the point C_i , fixed in this link, and the orthonormal basis \mathbf{e}^i ; $i = 1, \dots, n$, introduced above (Fig. 10). The relative motion in each hinge has only one degree of freedom and in this way the position of the mechanism is determined by m generalized parameters $\underline{q} = (q_1, \dots, q_m)^T$. We can write down for each pair of contiguous bodies the formula (Fig. 10)

$$(\mathbf{R}_{i+(a)} + \mathbf{c}_{i+(a)a}) - (\mathbf{R}_{i-(a)} + \mathbf{c}_{i-(a)a}) = -\mathbf{z}_a, \quad a = 1, \dots, m. \quad (4.1)$$

Taking into account the incidence matrix (2.1), we rewrite this relation in the following way:

$$\sum_{i=0}^n S_{ia} (\mathbf{R}_i + \mathbf{c}_{ia}) = S_{0a}\mathbf{c}_{0a} + \sum_{i=1}^n S_{ia} (\mathbf{R}_i + \mathbf{c}_{ia}) = -\mathbf{z}_a, \quad a = 1, \dots, m. \quad (4.2)$$

Let us define now with the help of the incidence matrix the following matrix

$$\underline{\mathbf{J}} = (S_{ia}\mathbf{c}_{ia}) \quad (i = 0, 1, \dots, n; a = 1, \dots, m), \quad (4.3)$$

where the vectors \mathbf{c}_{ia} are defined only for $i = i^\pm(a)$. We put them zero for the remaining indices. The last matrix has the same structure as the incidence matrix:

$$\underline{\mathbf{J}} = \begin{bmatrix} \underline{\mathbf{C}}_0 & \hat{\underline{\mathbf{C}}}_0 \\ \underline{\mathbf{C}} & \hat{\underline{\mathbf{C}}} \end{bmatrix} = \begin{bmatrix} \underline{\mathbf{C}}_0 \\ \underline{\mathbf{C}} \end{bmatrix},$$

where

$$\begin{aligned} \underline{\mathbf{C}}_0^{\vee} &= (S_{0a} \mathbf{c}_{0a}) \quad (a = 1, \dots, n), & \underline{\mathbf{C}}_0^{\wedge} &= (S_{0a} \mathbf{c}_{0a}) \quad (a = n + 1, \dots, m) \\ \underline{\mathbf{C}}^{\vee} &= (S_{ia} \mathbf{c}_{ia}) \quad (i, a = 1, \dots, n), & \underline{\mathbf{C}}^{\wedge} &= (S_{ia} \mathbf{c}_{ia}) \quad (i = 1, \dots, m; a = n + 1, \dots, m), \\ \underline{\mathbf{C}}_0 &= (S_{0a} \mathbf{c}_{0a}) \quad (a = 1, \dots, n), & \underline{\mathbf{C}} &= (S_{ia} \mathbf{c}_{ia}) \quad (i = 1, \dots, n; a = 1, \dots, m) \end{aligned}$$

We define in the same way the matrix

$$\underline{\mathbf{J}}^* = (S_{ia}^+ \mathbf{z}_a), \quad (i = 0, 1, \dots, n; a = 1, \dots, m) \quad (4.4)$$

where S_{ia}^+ are quantities defined in (2.2). The last matrix has the form

$$\underline{\mathbf{J}} = \begin{bmatrix} \underline{\mathbf{C}}_0^{\vee} & \underline{\mathbf{C}}_0^{\wedge} \\ \underline{\mathbf{C}}^{\vee} & \underline{\mathbf{C}}^{\wedge} \end{bmatrix} = \begin{bmatrix} \underline{\mathbf{C}}_0^* \\ \underline{\mathbf{C}}^* \end{bmatrix},$$

where

$$\begin{aligned} \underline{\mathbf{C}}_0^{\vee*} &= (S_{0a}^+ \mathbf{z}_a) \quad (a = 1, \dots, n), & \underline{\mathbf{C}}_0^{\wedge*} &= (S_{0a}^+ \mathbf{z}_a) \quad (a = n + 1, \dots, m), \\ \underline{\mathbf{C}}^{\vee*} &= (S_{ia}^+ \mathbf{z}_a) \quad (i, a = 1, \dots, n), & \underline{\mathbf{C}}^{\wedge*} &= (S_{ia}^+ \mathbf{z}_a) \quad (i = 1, \dots, n; a = n + 1, \dots, m), \\ \underline{\mathbf{C}}_0^* &= (S_{0a}^+ \mathbf{z}_a) \quad (a = 1, \dots, m), & \underline{\mathbf{C}}^* &= (S_{ia}^+ \mathbf{z}_a) \quad (i = 1, \dots, n; a = 1, \dots, m). \end{aligned}$$

The vector \mathbf{z}_a can be represented in the form:

$$\mathbf{z}_a = \sum_{i=0}^n S_{ia}^+ \mathbf{z}_a.$$

From here for the matrix $\underline{\mathbf{z}} = (\mathbf{z}_1, \dots, \mathbf{z}_m)^T$ follows the relation

$$\underline{\mathbf{z}} = (\underline{\mathbf{J}}^*)^T \underline{\mathbf{1}}_{n+1}, \quad (4.5)$$

where $\underline{\mathbf{1}}_{n+1}$ is a column $[(n + 1) \times 1]$ -matrix of unit elements. Now, defining $\underline{\mathbf{R}} = (\underline{\mathbf{R}}_1, \dots, \underline{\mathbf{R}}_n)^T$ we are able to represent (4.2) in the following form:

$$\underline{\mathbf{I}}^T \begin{bmatrix} \mathbf{0} \\ \underline{\mathbf{R}} \end{bmatrix} + \underline{\mathbf{J}}^T \underline{\mathbf{1}}_{n+1} = -\underline{\mathbf{z}}$$

or:

$$\underline{\mathbf{I}}^T \begin{bmatrix} \mathbf{0} \\ \underline{\mathbf{R}} \end{bmatrix} + (\underline{\mathbf{J}} + \underline{\mathbf{J}}^*)^T \underline{\mathbf{1}}_{n+1} = \underline{\mathbf{0}}_{m \times 1}. \quad (4.6)$$

Multiplying this relation from the left with $\underline{\Psi}^T$ and taking into account the relation [7]

$$\underline{\Psi}^T \underline{I}^T = (-1_n, \underline{E}_n),$$

Where \underline{E}_n is a unit $n \times n$ matrix, we find that

$$\underline{\mathbf{R}} = -\underline{\Psi}^T (\underline{\mathbf{J}} + \underline{\mathbf{J}}^*)^T \underline{1}_{n+1}. \quad (4.7)$$

This expression represents the radius-vectors \mathbf{R}_i ($i = 1, \dots, n$) of the points C_i fixed in the links with respect to the absolute coordinate system through the hinge vectors and eventually through the generalized parameters of the mechanism. Without loss of generality we can choose $C_0 = C_1$ and then $\mathbf{c}_{01} = \mathbf{0}$. Particularly, we have for the characteristic link

$$\mathbf{R}_{i^*} = \sum_{i=1}^{i^*} \mathbf{z}_i + \sum_{i=1}^{i^*-1} (\mathbf{c}_{i,i+1} - \mathbf{c}_{ii}). \quad (4.8)$$

The last relationship determines the radius-vector of point C_{i^*} of the characteristic link with respect to the absolute coordinate system. Outgoing from (4.8) and taking into account that the quantities \mathbf{c}_{ia} are identical for both mechanisms and the differences in the attitudes are due to the different values of the vectors \mathbf{z}_a in both mechanisms, we obtain the following expression for the deviation of the characteristic point

$$\Delta \mathbf{R}_{i^*} = \sum_{i=1}^{i^*} \Delta \mathbf{z}_i.$$

The matrices (4.3), (4.4) $\underline{\mathbf{J}}$ and $\underline{\mathbf{J}}^*$ for the four-bar mechanism have the following form (Fig. 2):

$$\underline{\mathbf{J}} = \begin{bmatrix} \mathbf{c}_{01} & \mathbf{0} & \mathbf{c}_{03} & \mathbf{0} \\ -\mathbf{c}_{11} & \mathbf{c}_{12} & \mathbf{0} & \mathbf{0} \\ \mathbf{0} & -\mathbf{c}_{22} & \mathbf{0} & \mathbf{c}_{24} \\ \mathbf{0} & \mathbf{0} & -\mathbf{c}_{34} & -\mathbf{c}_{34} \end{bmatrix}, \quad \underline{\mathbf{J}}^* = \begin{bmatrix} \mathbf{z}_1 & \mathbf{0} & \mathbf{z}_3 & \mathbf{0} \\ \mathbf{0} & \mathbf{z}_2 & \mathbf{0} & \mathbf{0} \\ \mathbf{0} & \mathbf{0} & \mathbf{0} & \mathbf{z}_4 \\ \mathbf{0} & \mathbf{0} & \mathbf{0} & \mathbf{0} \end{bmatrix}.$$

The formula (4.7) is now

$$\begin{bmatrix} \mathbf{R}_1 \\ \mathbf{R}_2 \\ \mathbf{R}_3 \end{bmatrix} = \begin{bmatrix} \mathbf{z}_1 + \mathbf{c}_{01} - \mathbf{c}_{11} \\ \mathbf{z}_1 + \mathbf{z}_2 + \mathbf{c}_{01} + \mathbf{c}_{12} - \mathbf{c}_{11} - \mathbf{c}_{22} \\ \mathbf{z}_3 + \mathbf{c}_{03} - \mathbf{c}_{33} \end{bmatrix}.$$

The radius-vector \mathbf{R}_C of the characteristic point (coupler point) C is (Fig. 2)

$$\mathbf{R}_C = \mathbf{R}_1 + r_3 \mathbf{e}_1^{(2)}$$

and

$$\Delta \mathbf{R}_C = \Delta \mathbf{R}_1 = \Delta \mathbf{z}_1$$

Let us consider now the second example. For the six-bar mechanism the matrices (4.3), (4.4) $\underline{\mathbf{J}}$ and $\underline{\mathbf{J}}^*$ are (Fig. 4):

$$\underline{\mathbf{J}} = \begin{bmatrix} \mathbf{c}_{01} & \mathbf{0} & \mathbf{c}_{03} & \mathbf{0} & \mathbf{0} & \mathbf{0} & \mathbf{0} \\ -\mathbf{c}_{11} & \mathbf{c}_{12} & \mathbf{0} & \mathbf{0} & \mathbf{0} & \mathbf{c}_{16} & \mathbf{0} \\ \mathbf{0} & -\mathbf{c}_{22} & \mathbf{0} & \mathbf{0} & \mathbf{0} & \mathbf{0} & \mathbf{c}_{27} \\ \mathbf{0} & \mathbf{0} & -\mathbf{c}_{33} & \mathbf{c}_{34} & \mathbf{c}_{35} & \mathbf{0} & \mathbf{0} \\ \mathbf{0} & \mathbf{0} & \mathbf{0} & -\mathbf{c}_{44} & \mathbf{0} & \mathbf{0} & -\mathbf{c}_{47} \\ \mathbf{0} & \mathbf{0} & \mathbf{0} & \mathbf{0} & -\mathbf{c}_{55} & -\mathbf{c}_{56} & \mathbf{0} \end{bmatrix},$$

$$\underline{\mathbf{J}}^* = \begin{bmatrix} \mathbf{z}_1 & \mathbf{0} & \mathbf{z}_3 & \mathbf{0} & \mathbf{0} & \mathbf{0} & \mathbf{0} \\ \mathbf{0} & \mathbf{z}_2 & \mathbf{0} & \mathbf{0} & \mathbf{0} & \mathbf{z}_6 & \mathbf{0} \\ \mathbf{0} & \mathbf{0} & \mathbf{0} & \mathbf{0} & \mathbf{0} & \mathbf{0} & \mathbf{z}_7 \\ \mathbf{0} & \mathbf{0} & \mathbf{0} & \mathbf{z}_4 & \mathbf{z}_5 & \mathbf{0} & \mathbf{0} \\ \mathbf{0} & \mathbf{0} & \mathbf{0} & \mathbf{0} & \mathbf{0} & \mathbf{0} & \mathbf{0} \\ \mathbf{0} & \mathbf{0} & \mathbf{0} & \mathbf{0} & \mathbf{0} & \mathbf{0} & \mathbf{0} \end{bmatrix}.$$

The expression (4.7) has the form

$$\begin{bmatrix} \mathbf{R}_1 \\ \mathbf{R}_2 \\ \mathbf{R}_3 \\ \mathbf{R}_4 \\ \mathbf{R}_5 \end{bmatrix} = \begin{bmatrix} \mathbf{c}_{01} + \mathbf{z}_1 - \mathbf{c}_{11} \\ \mathbf{z}_1 + \mathbf{z}_2 + \mathbf{c}_{01} - \mathbf{c}_{11} + \mathbf{c}_{12} - \mathbf{c}_{22} \\ \mathbf{c}_{03} + \mathbf{z}_3 - \mathbf{c}_{33} \\ \mathbf{z}_3 + \mathbf{z}_4 - \mathbf{c}_{33} + \mathbf{c}_{03} + \mathbf{c}_{34} - \mathbf{c}_{44} \\ \mathbf{z}_3 + \mathbf{z}_5 + \mathbf{c}_{03} + \mathbf{c}_{35} - \mathbf{c}_{33} - \mathbf{c}_{55} \end{bmatrix}.$$

Choosing point D as a characteristic point we have for its radius vector the expression (Fig. 4)

$$\mathbf{R}_D = \mathbf{R}_2 + h\mathbf{e}_1^{(2)}, \quad h = |\overline{CD}|,$$

or

$$\mathbf{R}_D = \mathbf{z}_1 + \mathbf{z}_2 + \mathbf{c}_{01} - \mathbf{c}_{11} + \mathbf{c}_{12} - \mathbf{c}_{22},$$

and finally

$$\Delta \mathbf{R}_D = \Delta \mathbf{R}_2 = \Delta \mathbf{z}_1 + \Delta \mathbf{z}_2.$$

The matrices (4.3), (4.4) $\underline{\mathbf{J}}$ and $\underline{\mathbf{J}}^*$ in the last example – the nine-bar mechanism (Fig. 6) are:

$$\underline{\mathbf{J}} = \begin{bmatrix} c_{01} & 0 & 0 & 0 & 0 & 0 & 0 & 0 & c_{09} & c_{010} \\ -c_{11} & c_{12} & 0 & 0 & 0 & 0 & 0 & 0 & 0 & 0 \\ 0 & -c_{22} & c_{23} & 0 & 0 & 0 & 0 & 0 & 0 & 0 \\ 0 & 0 & -c_{33} & c_{34} & 0 & 0 & c_{37} & 0 & 0 & 0 \\ 0 & 0 & 0 & -c_{44} & c_{45} & 0 & 0 & 0 & 0 & 0 \\ 0 & 0 & 0 & 0 & -c_{55} & c_{56} & 0 & 0 & 0 & 0 \\ 0 & 0 & 0 & 0 & 0 & -c_{66} & 0 & 0 & -c_{68} & 0 \\ 0 & 0 & 0 & 0 & 0 & 0 & -c_{77} & c_{78} & 0 & 0 \\ 0 & 0 & 0 & 0 & 0 & 0 & 0 & -c_{88} & 0 & -c_{810} \end{bmatrix},$$

$$\underline{\mathbf{J}}^* = \begin{bmatrix} z_1 & 0 & 0 & 0 & 0 & 0 & 0 & 0 & z_9 & z_{10} \\ 0 & z_2 & 0 & 0 & 0 & 0 & 0 & 0 & 0 & 0 \\ 0 & 0 & z_3 & 0 & 0 & 0 & 0 & 0 & 0 & 0 \\ 0 & 0 & 0 & z_4 & 0 & 0 & z_7 & 0 & 0 & 0 \\ 0 & 0 & 0 & 0 & z_5 & 0 & 0 & 0 & 0 & 0 \\ 0 & 0 & 0 & 0 & 0 & z_6 & 0 & 0 & 0 & 0 \\ 0 & 0 & 0 & 0 & 0 & 0 & 0 & 0 & 0 & 0 \\ 0 & 0 & 0 & 0 & 0 & 0 & 0 & z_8 & 0 & 0 \\ 0 & 0 & 0 & 0 & 0 & 0 & 0 & 0 & 0 & 0 \end{bmatrix}.$$

The formula (4.7) takes the form:

$$\begin{bmatrix} \mathbf{R}_1 \\ \mathbf{R}_2 \\ \mathbf{R}_3 \\ \mathbf{R}_4 \\ \mathbf{R}_5 \\ \mathbf{R}_6 \\ \mathbf{R}_7 \\ \mathbf{R}_8 \end{bmatrix} = \begin{bmatrix} z_1 + c_{01} - c_{11} \\ z_1 + z_2 + c_{01} + c_{12} - c_{11} - c_{22} \\ z_1 + z_2 + z_3 + c_{01} + c_{12} + c_{23} - c_{11} - c_{22} - c_{33} \\ z_1 + z_2 + z_3 + z_4 + c_{01} + c_{12} + c_{23} + c_{34} - c_{11} - c_{22} - c_{33} - c_{44} \\ z_1 + z_2 + z_3 + z_4 + z_5 + c_{01} + c_{12} + c_{23} + c_{34} + c_{45} - c_{11} - c_{22} - c_{33} - c_{44} - c_{55} \\ z_1 + z_2 + z_3 + z_4 + z_5 + z_6 + c_{01} + c_{12} + c_{23} + c_{34} + c_{45} + c_{36} - \left(\sum_{i=1}^6 c_{ii} \right) \\ z_1 + z_2 + z_3 + z_7 + c_{01} + c_{12} + c_{23} + c_{37} - c_{11} - c_{22} - c_{33} - c_{77} \\ z_1 + z_2 + z_3 + z_7 + z_8 + c_{01} + c_{12} + c_{23} + c_{37} + c_{78} - c_{11} - c_{22} - c_{33} - c_{77} - c_{88} \end{bmatrix}$$

Choosing point F as a characteristic point we have for the position vector the expression (Fig. 6)

$$\mathbf{R}_F = \mathbf{R}_2 + h_1 \mathbf{e}_1^{(2)}, \quad |BF| = h_1,$$

or

$$\Delta \mathbf{R}_F = \Delta \mathbf{R}_2 = \Delta z_1 + \Delta z_2.$$

5. CONSTRAINT EQUATIONS

The availability of loops in the considered mechanisms leads to the appearance of constraints between the generalized parameters q_a imposed on the mutual motion of the links forming a system of fundamental loops. Each of the fundamental loops imposes 3 scalar constraints independent of the remaining loops. These constraints express the trivial circumstance that the radius-vector of the origin of one (no matter which) of the coordinate systems fixed in the links of the loop with respect to this origin is the zero vector and, similarly, that the angular position of this coordinate system with respect to itself is given by the unit matrix. Following from an arbitrary link of the loop in one direction and expressing these quantities through the coordinate systems of the passed links, we find a formal record of the constraints after accomplishing the cycle. Let us derive first the constraint connected with the angular attitude of the links of the loop considered. Let the loop Φ_a consist of arcs u_{b_1}, \dots, u_{b_a} ($a = n + 1, \dots, m$) and the sense of direction is determined by the direction of the arc u_{b_a} . Let i and j be the contiguous links for the hinge number b_k and let α be the angle between the x -axes of the coordinate systems fixed in the contiguous links. Obviously, if the link i is chosen as a reference link and the value of the parameter q_{b_k} is α , then the value of q_{b_k} will be $(-\alpha)$ if the link j is chosen as a reference link. Therefore, starting the calculation from an arbitrary link we find that the constraint, imposed by the loop, will have the form

$$q_{j_1} + q_{j_2} + \dots + q_{j_{n_1}} = q_{k_1} + q_{k_2} + \dots + q_{k_{n_2}}, \quad (5.1)$$

where j_1, \dots, j_{n_1} are the numbers of the arcs with the same sense of direction as the arc u_{b_a} and k_1, \dots, k_{n_2} are the numbers of the arcs with the opposite sense of direction.

This result can be obtained in a formal way, as well. Let the transition matrix in hinge b_k be \underline{G}_{b_k} and let the link number i be chosen as a reference body. Let the value of the parameter q_{b_k} be α , then the matrix \underline{G}_{b_k} has the form:

$$\underline{G}_{b_k} = \underline{\mathbf{e}}^{(i)} \cdot \underline{\mathbf{e}}^{(j)T} = \begin{bmatrix} \cos \alpha & -\sin \alpha \\ \sin \alpha & \cos \alpha \end{bmatrix}.$$

If we choose as a reference link the contiguous link, then the value of q_{b_k} is $(-\alpha)$ and the transition matrix is $\underline{G}_{b_k}^{-1} = \underline{G}_{b_k}^T$. Outgoing from the definition (2.3) for the quantities φ_{ab} we can write down the relation

$$\underline{G}_{b_1}^{\varphi_{ab_1}}, \underline{G}_{b_2}^{\varphi_{ab_2}}, \dots, \underline{G}_{b_a}^{\varphi_{ab_a}} = \underline{E}_2 \quad (a = n + 1, \dots, m), \quad (5.2)$$

where \underline{E}_2 is 2×2 unit matrix. Each of the matrices in this relation is an antisymmetric one. It is an easy task to prove that the product of two antisymmetric matrices is commutative

$$\begin{bmatrix} a_1 & b_1 \\ -b_1 & a_1 \end{bmatrix} \begin{bmatrix} a_2 & b_2 \\ -b_2 & a_2 \end{bmatrix} = \begin{bmatrix} a_2 & b_2 \\ -b_2 & a_2 \end{bmatrix} \begin{bmatrix} a_1 & b_1 \\ -b_1 & a_1 \end{bmatrix}.$$

Consequently, in the left side of (5.2) we can first write down the matrices with positive exponents φ_{ab} and then – those with negative exponents. The product of the former matrices has the form

$$\begin{bmatrix} \cos(q_{j_1} + q_{j_2} + \dots + q_{j_{n_1}}) & -\sin(q_{j_1} + q_{j_2} + \dots + q_{j_{n_1}}) \\ \sin(q_{j_1} + q_{j_2} + \dots + q_{j_{n_1}}) & \cos(q_{j_1} + q_{j_2} + \dots + q_{j_{n_1}}) \end{bmatrix},$$

and the product of the latter – the form

$$\begin{bmatrix} \cos(q_{k_1} + q_{k_2} + \dots + q_{k_{n_2}}) & \sin(q_{k_1} + q_{k_2} + \dots + q_{k_{n_2}}) \\ -\sin(q_{k_1} + q_{k_2} + \dots + q_{k_{n_2}}) & \cos(q_{k_1} + q_{k_2} + \dots + q_{k_{n_2}}) \end{bmatrix}.$$

After multiplying these matrices the relation (5.2) obtains the form:

$$\begin{bmatrix} \cos \left[\left(\sum_{i=1}^{n_1} q_{j_i} \right) - \left(\sum_{i=1}^{n_2} q_{k_i} \right) \right] & \sin \left[\left(\sum_{i=1}^{n_1} q_{j_i} \right) - \left(\sum_{i=1}^{n_2} q_{k_i} \right) \right] \\ -\sin \left[\left(\sum_{i=1}^{n_1} q_{j_i} \right) - \left(\sum_{i=1}^{n_2} q_{k_i} \right) \right] & \cos \left[\left(\sum_{i=1}^{n_1} q_{j_i} \right) - \left(\sum_{i=1}^{n_2} q_{k_i} \right) \right] \end{bmatrix} = \begin{bmatrix} 1 & 0 \\ 0 & 1 \end{bmatrix}$$

what leads us again to the relation (5.1).

The remaining two constraints express the equality to zero of the radius-vector of an arbitrary origin with respect to itself, or in other words, the radius-vector of the coordinate origin of the link chosen as an initial one, expressed through the sequence of vectors $\mathbf{c}_{i\pm(a)}$ and \mathbf{z}_a along the arcs u_a belonging to the considered loop, is equal to zero. We can find these constraints by multiplying the relationship (4.6) from left with the cyclomatic matrix $\underline{\Phi}$ following [7]. We find, after simple calculations, the formula

$$\underline{\Phi} \mathbf{J}^T \mathbf{1}_{n+1} + \underline{\Phi} \mathbf{z} = \mathbf{0}_{\hat{n} \times 1}.$$

Using (4.5) we rewrite this relation in the form

$$\underline{\Phi} \mathbf{J}^T \mathbf{1}_{n+1} + \underline{\Phi} \mathbf{z} = \mathbf{0}_{\hat{n} \times 1}.$$

This relationship is fulfilled for both mechanisms, therefore

$$\underline{\Phi}(\underline{\mathbf{J}} - \underline{\mathbf{J}}^r)^T \mathbf{1}_{n+1} + \underline{\Phi} \Delta \mathbf{z} = \mathbf{0}_{\hat{n} \times 1}$$

The vectors \mathbf{c}_{ia} have identical values for both mechanisms, i.e. $\underline{\mathbf{J}} = \underline{\mathbf{J}}^r$ and finally

$$\underline{\Phi} \Delta \mathbf{z} = \mathbf{0}_{\hat{n} \times 1}. \quad (5.3)$$

Projecting (5.3) on the axes x and y in the motion plane we obtain $2\hat{n}$ scalar relations which are the constrain equations together with (5.1).

As an example, let us consider again the four-bar mechanism. We have only one loop and the equations (5.3) are now (Fig. 2)

$$\begin{aligned} r_2 \cos q_1 + r_6 \cos(q_1 + q_2) - r_4 \cos q_3 - r_1 &= 0 \\ r_2 \sin q_1 + r_6 \sin(q_1 + q_2) - r_4 \sin q_3 &= 0. \end{aligned} \quad (5.4)$$

On the other hand, the relation (5.4) takes the form

$$q_1 + q_2 - q_3 + q_4 = 0. \quad (5.5)$$

From (5.4) we obtain

$$q_3 = \arctan \left(\frac{r_2 \sin q_1 + r_6 \sin(q_1 + q_2)}{r_2 \cos q_1 + r_6 \cos(q_1 + q_2) - r_1} \right). \quad (5.6)$$

Eliminating q_3 by squaring and adding the equations (5.4), we get

$$r_4^2 - (r_1^2 + r_2^2 + r_6^2) = 2r_2r_6 \cos q_2 - 2r_1r_2 \cos q_1 - 2r_1r_6 \cos(q_1 + q_2).$$

This formula allows representing q_2 as a function of q_1 and further q_3 and q_4 through (5.6) and (5.5). Finally the constraint equations (5.3) have the form

$$\begin{bmatrix} 1 & 1 & -1 & 1 \end{bmatrix} \begin{bmatrix} \Delta z_1 \\ \Delta z_2 \\ \Delta z_3 \\ \Delta z_4 \end{bmatrix} = \mathbf{0}$$

or

$$\Delta z_1 + \Delta z_2 - \Delta z_3 + \Delta z_4 = 0.$$

Let us now find the parameters of the displacement for the six-bar mechanism through the generalized parameters $q_1, q_2, q_3, q_4, q_5, q_6$ and q_7 (Fig. 4). To that end, we use the loop-closure equations. The loop-closure equations of first four-bar linkage $O_A A B O_B$ are written as:

$$\begin{aligned} a \cos(q_1 - \alpha) - b \cos(q_1 + q_6) - c \cos(q_3 + \beta) - d &= 0 \\ a \sin(q_1 - \alpha) - b \sin(q_1 + q_6) - c \sin(q_3 + \beta) &= 0 \end{aligned} \quad (5.7)$$

$$q_1 - q_3 - q_5 + q_6 = 0, \quad (5.8)$$

where $\alpha = \angle(\overline{O_A A}, \overline{O_A C})$, $\beta = \angle(\overline{O_B E}, \overline{O_B B})$, $a = |O_A A|$, $b = |AB|$, $c = |O_B B|$, $d = |O_A O_B|$. From (5.7) we get the formula

$$q_3 = \arctan \left(\frac{a \sin(q_1 - \alpha) - b \sin(q_1 + q_6)}{a \cos(q_1 - \alpha) - b \cos(q_1 + q_6) - d} \right) - \beta. \quad (5.9)$$

In order to get rid of the angle q_3 in (5.7), we square and add the equations. We obtain

$$c^2 - (a^2 + b^2 + d^2) = -2ab \cos(q_6 + \alpha) - 2ad \cos(q_1 - \alpha) + 2bd \cos(q_1 + q_6). \quad (5.10)$$

As q_1 is the input data and can be chosen as a generalized coordinate, then q_6 is determined from (5.10) as a function of q_1 , hence q_3 through (5.9) is a function of q_1 . The relation (5.8) gives finally $q_5 = q_1 - q_3 - q_6$ as a function of q_1 .

The closure equations for the second loop – the five-bar linkage $O_A C D E O_B$ are given as:

$$\begin{aligned} e \cos q_1 + h \cos(q_1 + q_2) - g \cos(q_3 + q_4) - f \cos q_3 - d &= 0 \\ e \sin q_1 + h \sin(q_1 + q_2) - g \sin(q_3 + q_4) - f \sin q_3 &= 0 \end{aligned} \quad (5.11)$$

$$q_1 + q_2 - q_3 - q_4 + q_7 = 0 \quad (5.12)$$

where $e = |O_A C|$, $f = |O_B E|$, $g = |ED|$ and $h = |CD|$ are dimensions of the six-bar Stephenson-I mechanism.

After squaring and adding the equations (5.11) we obtain

$$\begin{aligned} h^2 - (d^2 + e^2 + f^2 + g^2) &= -2eg \cos[q_1 - (q_3 + q_4)] - 2ef \cos(q_1 + q_3) + 2fg \cos q_4 \\ &\quad - 2de \cos q_1 + 2dg \cos(q_3 + q_4) + 2df \cos q_3. \end{aligned} \quad (5.13)$$

From (5.11) we get

$$q_2 = -q_1 + \arctan \frac{e \sin q_1 - g \sin(q_3 + q_4) - f \sin q_3}{e \cos q_1 - g \cos(q_3 + q_4) - f \cos q_3 - d}. \quad (5.14)$$

The parameter q_4 can be expressed from equation (5.13) as a function of the generalized coordinate q_1 . The generalized parameter q_2 is expressed as function of q_1 from (5.14). Finally, the last parameter q_7 can be derived as a function of q_1 from (5.12).

The constraint equations (5.3) for this mechanism have the form

$$\begin{aligned} \Delta \mathbf{z}_1 - \Delta \mathbf{z}_3 - \Delta \mathbf{z}_5 + \Delta \mathbf{z}_6 &= \mathbf{0} \\ \Delta \mathbf{z}_1 + \Delta \mathbf{z}_2 - \Delta \mathbf{z}_3 - \Delta \mathbf{z}_4 + \Delta \mathbf{z}_7 &= \mathbf{0}. \end{aligned}$$

The nine-bar mechanism has nine links and ten revolute joints, consequently 10 generalized parameters q_i ($i = 1, \dots, 10$) (Fig. 6). As the mechanism has two independent loops, the number of the degrees of freedom is four. We choose as generalized coordinates the first generalized parameters q_i ($i = 1, \dots, 4$). We have from the loop ($OABFGHI$), the following constraint equations:

$$q_1 + q_2 + q_3 + q_4 + q_5 + q_6 - q_9 = 0 \quad (5.15)$$

$$\begin{aligned} b_1 \cos q_1 + b_2 \cos(q_1 + q_2) + h_1 \cos(q_1 + q_2 + q_3) + \\ b_4 \cos \left(\sum_{i=1}^4 q_i \right) + b_5 \cos \left(\sum_{i=1}^5 q_i \right) + b_6 \cos q_9 - a &= 0 \\ b_1 \sin q_1 + b_2 \sin(q_1 + q_2) + h_1 \sin(q_1 + q_2 + q_3) + \\ b_4 \sin \left(\sum_{i=1}^4 q_i \right) + b_5 \sin \left(\sum_{i=1}^5 q_i \right) + b_6 \sin q_9 &= 0, \end{aligned} \quad (5.16)$$

where $h_1 = BF$. From relation (5.16) we get

$$\arctan \left[\frac{b_1 \cos q_1 + b_2 \cos(q_1 + q_2) + h_1 \cos \left(\sum_{i=1}^3 q_i \right) + b_4 \cos \left(\sum_{i=1}^4 q_i \right) + b_5 \cos \left(\sum_{i=1}^5 q_i \right) - a}{b_1 \sin q_1 + b_2 \sin(q_1 + q_2) + h_1 \sin \left(\sum_{i=1}^3 q_i \right) + b_4 \sin \left(\sum_{i=1}^4 q_i \right) + b_5 \sin \left(\sum_{i=1}^5 q_i \right)} \right] \quad (5.17)$$

Now, adding after squaring the equations (5.16), we get

$$\begin{aligned} b_7^2 - (b_1^2 + b_2^2 + h_1^2 + b_4^2 + b_5^2 + a^2) = & \\ & 2b_1b_2 \cos q_2 + 2b_1h_1 \cos(q_2 + q_3) + 2b_1b_4 \cos \left(\sum_{i=2}^4 q_i \right) \\ & + 2b_1b_5 \cos \left(\sum_{i=2}^5 q_i \right) + 2b_2h_1 \cos q_3 + 2b_2b_4 \cos(q_3 + q_4) \\ & + 2b_2b_5 \cos \left(\sum_{i=3}^5 q_i \right) + 2h_1b_4 \cos q_4 + 2h_1b_5 \cos(q_4 + q_5) \\ & + 2b_4b_5 \cos q_5 - 2ab_1 \cos q_1 - 2ab_2 \cos(q_1 + q_2) \\ & - 2ah_1 \cos \left(\sum_{i=1}^3 q_i \right) - 2ab_4 \cos \left(\sum_{i=1}^4 q_i \right) - 2ab_5 \cos \left(\sum_{i=1}^5 q_i \right). \end{aligned}$$

This relation determines generalized parameter q_5 as a function of the generalized coordinates, $q_5 = h(q_1, q_2, q_3, q_4)$. Hence, from (5.17) we have $q_9 = f(q_1, q_2, q_3, q_4)$ and from (5.15) we get $q_6 = g(q_1, q_2, q_3, q_4)$.

The second loop ($OABCDE$) delivers the equations (Fig. 6)

$$q_1 + q_2 + q_3 + q_7 + q_8 - q_{10} = 0 \quad (5.18)$$

$$\begin{aligned} b_1 \cos q_1 + b_2 \cos(q_1 + q_2) + b_3 \cos \left(\sum_{i=1}^3 q_i \right) + b_7 \cos \left(q_7 + \sum_{i=1}^3 q_i \right) + b_8 \cos q_{10} - c &= 0 \\ b_1 \sin q_1 + b_2 \sin(q_1 + q_2) + b_3 \sin \left(\sum_{i=1}^3 q_i \right) + b_7 \sin \left(q_7 + \sum_{i=1}^3 q_i \right) + b_8 \sin q_{10} &= 0. \end{aligned} \quad (5.19)$$

From (5.19) we obtain the relations

$$q_{10} = \arctan \left[\frac{b_1 \sin q_1 + b_2 \sin(q_1 + q_2) + b_3 \sin \left(\sum_{i=1}^3 q_i \right) + b_7 \sin \left(q_7 + \sum_{i=1}^3 q_i \right)}{b_1 \cos q_1 + b_2 \cos(q_1 + q_2) + b_3 \cos \left(\sum_{i=1}^3 q_i \right) + b_7 \cos \left(q_7 + \sum_{i=1}^3 q_i \right) - c} \right], \quad (5.20)$$

$$\begin{aligned}
b_7^2 - (b_1^2 + b_2^2 + b_3^2 + b_4^2 + b_5^2 + a^2) = \\
2b_1b_2 \cos q_2 + 2b_1b_3 \cos(q_2 + q_3) + 2b_1b_7 \cos(q_2 + q_3 + q_7) \\
+ 2b_2b_3 \cos q_3 + 2b_2b_7 \cos(q_3 + q_7) + 2b_3b_7 \cos q_7 \\
+ 2b_3b_4 \cos q_4 + 2b_3b_5 \cos(q_4 + q_5) - 2b_1c \cos q_1 \\
- 2b_2c \cos(q_1 + q_2) - 2b_3c \cos\left(\sum_{i=1}^3 q_i\right) - 2b_7c \cos\left(q_7 + \sum_{i=1}^3 q_i\right).
\end{aligned}$$

The last relation determines the generalized parameter q_7 as a function of three generalized coordinates, $q_7 = h_1(q_1, q_2, q_3)$. Hence, from (5.20) we have $q_{10} = f_1(q_1, q_2, q_3)$ and further from (5.18) we get $q_8 = g_1(q_1, q_2, q_3)$.

The relations (5.3) for the planar platform are:

$$\begin{aligned}
-(\Delta z_1 + \Delta z_2 + \Delta z_3 + \Delta z_4 + \Delta z_5 + \Delta z_6) + \Delta z_9 &= 0 \\
-(\Delta z_1 + \Delta z_2 + \Delta z_3 + \Delta z_7 + \Delta z_8) + \Delta z_{10} &= 0
\end{aligned}$$

6. CONCLUSIONS

The displacement of the mechanism with super elastic hinges is compared with the displacement of the mechanism with traditional joints, considered as an ideal system. Using the graph theory a mathematical model is suggested and compact analytical expressions are given allowing an exact estimation of the deflections in links positions of the mechanism with super elastic hinges. The results obtained are applied on three famous mechanisms widely used in technics.

REFERENCES

1. Howell, L. Compliant Mechanisms. John Wiley&Sons, Inc. New York, 2002.
2. Kota, S., J. Joo, Z. Li, S. M. Rodgers, J. Sniegowski. *Design of compliant mechanisms: Application to MEMS*. Kluwer Academic Publishers. Manufactured in Netherlands, **29**, 2001, 7-15.
3. Lobontiu, N. Compliant Mechanisms. CRC Press, Boca Raton-London-New York-Washington, D.C., 2002.
4. Xu, G., L. Qu. Some analytical problems of high performance flexure hinge and Micro-motion stage design. In: *Proceedings the IEEE International Conference on Industrial Technology*, 1996, 771-775.
5. Lobontiu, N., J. S. N. Paine, E. O'Malley, M. Samuelson. Parabolic and hyperbolic flexure hinges: flexibility, motion precision and stress characterization based on compliance closed-form equations. *Precision Engineering, Journal of the International Societies for Precision Engineering and Nanotechnology*, **26**, 2002, 183-192.

6. Horie, M., T. Nozaki, K. Ikegami, F. Kobayashi. Design System of Superelastic Hinges and Its Application to Micromanipulators. *JSME International Journal, Series C*, **40**, 1997, 323–328.
7. Lilov, L. Modeling of multibody systems, Nauka, Moscow, 1993 (in Russian).
8. Christofides, N. Graph Theory: An Algorithmic Approach. Academic Press, New York, London, San Francisco, 1975.

Received on February 20, 2006

Faculty of Mathematics and Informatics
“St. Kl. Ohridski” University of Sofia
5, J. Bourchier blvd., 1164 Sofia
BULGARIA
E-mail: ktfpuswe@yahoo.com
E-mail: lilov@fmi.uni-sofia.bg